JOURNAL OF MATERIALS SCIENCE **39** (2004) 1647– 1652

Creep properties of a fiber-reinforced magnesium alloy

V. SKLENIČKA
Institute of Physics of Materials, Academy of Sciences of the Czech Republic, Žižkova 22, CZ-616 62 Brno, Czech Republic

T. G. LANGDON
Departments of Aerospace & Mechanical Engineering and Materials Science, University of Southern California, Los Angeles, CA 90089-1453, USA
E-mail: Langdon@usc.edu

There are both similarities and differences between the creep behavior of f.c.c. metals and an h.c.p. metal such as magnesium. This paper examines these differences and examines the additional creep strengthening that may be introduced in a commercial magnesium alloy such as AZ91 through the introduction of an array of short alumina fibers.
© *2004 Kluwer Academic Publishers*

1. Introduction

Magnesium is the lightest common metal so that magnesium-based alloys make excellent light-weight constructional materials. The characteristics of these alloys include a low density, good machinability, excellent recycling capabilities and damping capacities that are exceptionally high by comparison with all other materials [1]. As a consequence of these attributes, magnesium alloys are now under very serious consideration for a wide range of applications in the automotive field [2–4]. In addition, and especially as a consequence of the current need to reduce fuel consumption and CO_2 emissions in the automobile industry, there are predictions that we are about to enter a "new age of magnesium" [5].

Despite these advantages, the creep properties of magnesium-based alloys are generally inferior to those of the more conventional aluminum-based alloys. Attempts have been made to achieve better creep resistance through the development either of special creep-resistant alloys based on, for example, the MgSc and MgGd ternary systems [6] or through the production of composite materials where the matrices consist of conventional magnesium alloys which are strengthened through the introduction of fibers or particulates [7]. The present paper describes the results obtained in an investigation that was undertaken to explore the potential for introducing significant creep strengthening into an AZ91 magnesium alloy through the presence of 20 vol% of alumina short fibers. Several earlier reports described some of the creep data obtained with this and other comparable Mg-based materials [8–11] and the present paper builds on these results, supplements them with additional data, and then presents an analysis of the creep properties of the AZ91 metal matrix composite.

To place this paper in perspective, the following section provides a brief comparison of the creep behavior of f.c.c. and h.c.p. metals and the subsequent sections describe the experimental material and the results obtained in a comprehensive investigation of the creep behavior.

2. Creep properties of h.c.p. metals: a comparison with f.c.c. metals

Prior to examining creep data obtained for magnesium composites, it is first necessary to consider the fundamental creep properties of magnesium and Mg-based solid solution alloys since their h.c.p. crystal structure limits the availability of easy slip and this limitation is especially significant by comparison with metals, such as aluminum, where there is an f.c.c. crystal structure. Creep experiments on pure Mg at temperatures up to ~600 K have shown that, as in f.c.c. metals, the steady-state creep rate is related to the applied stress through a power-law in which the stress exponent is ~1 at very low stresses, ~5 over a wide range of intermediate stresses and with a breakdown in the power-law behavior at very high stresses [12]. All of these transitions are consistent with conventional theory [13] and they have been interpreted in terms of transitions from diffusion creep at the lowest stresses, dislocation climb with basal slip at intermediate stresses and power-law breakdown at very high stresses, where the diffusion creep and dislocation climb regions have activation energies of ~135 kJ mol^{-1} which is equal to the value for lattice self-diffusion in magnesium. The behavior at temperatures up to ~600 K is therefore similar to f.c.c. metals but at higher temperatures, above ~650 K, the power-law region at intermediate stresses has a slightly higher stress exponent of ~6, there is extensive non-basal slip, the activation energy becomes high and dependent on the level of the applied stress and the rate-controlling mechanism appears to be the cross-slip of dislocations from the basal to the prismatic planes [12].

In Mg-based solid solution alloys, experiments show that, as in f.c.c. solid solutions [14, 15], the viscous glide of dislocations is rate-controlling due to the presence of solute atom atmospheres around the moving dislocations and at the higher testing temperatures there is a high activation energy due to the cross-slip of dislocations to the prismatic planes [16]. Thus, these results reveal both similarities and differences between the creep of metals and metallic alloys having h.c.p. and f.c.c. crystal structures.

3. Experimental material and procedures

For comparison purposes, the experiments were conducted using two different materials: a conventional AZ91 alloy (Mg-9 wt% Al-1 wt% Zn-0.3 wt% Mn) and an AZ91 alloy reinforced with 20 vol% of δ-Al_2O_3 fibers, where the composite is henceforth designated AZ91-20 vol%Al_2O_3(f) where f denotes fibers. The reinforcing alumina fibers used for the composite had diameters of the order of $\sim$3 μm, varying lengths up to a maximum of $\sim$150 μm and their compositions were 97% Al_2O_3 and 3% SiO_2. The composite was fabricated using squeeze casting with an alumina binder and in the as-cast condition it was found through microscopic inspection that the fibers were arranged in a two-dimensional array but with random orientations within this array. The optical micrographs in Fig. 1a and b show the fiber distributions in two mutually perpendicular planes of sectioning. Prior to creep testing, the unreinforced AZ91 alloy and the AZ91 composite were subjected to a T6 heat treatment in which they were annealed for 6 h at 803 K, air cooled, and then aged for 8 h at 477 K. The initial grain size in the unreinforced alloy was measured as $\sim$200 μm as illustrated in Fig. 2. A detailed description of the material was given in an earlier report [11].

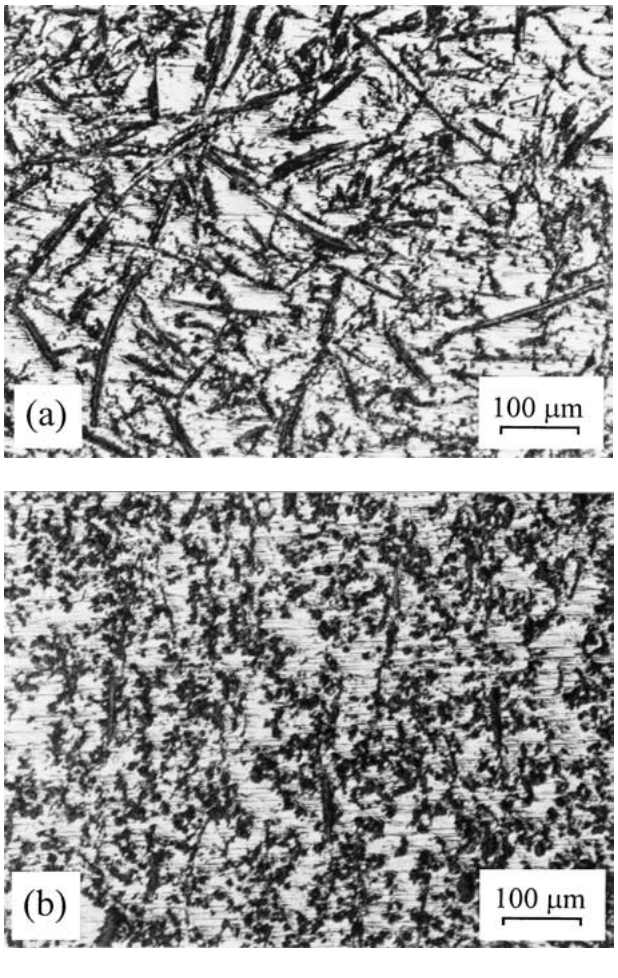

Figure 1 (a) and (b) Optical micrographs showing fiber distributions in the composite in two mutually perpendicular directions.

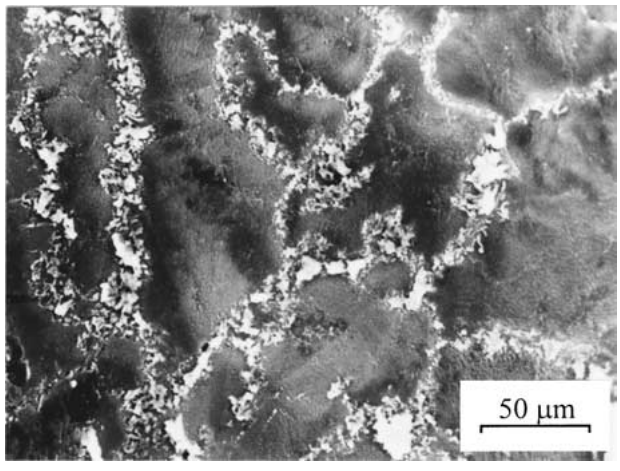

Figure 2 Optical micrograph showing microstructure of the unreinforced AZ91 alloy.

Creep tests were conducted in tension using samples having gauge lengths of 25 mm and cross-sectional areas of 3 $\times$ 3.2 mm. Each specimen was machined so that the longitudinal axis was parallel to the plane containing the two-dimensional array of fibers. The creep testing was conducted in an environment of purified argon under conditions of constant stress at temperatures of 423 and 473 K with the testing temperatures maintained to within $\pm$0.5 K of the desired value. Most of the tests were continued until fracture.

Metallographic inspection was conducted after creep testing using either a Philips CM12 transmission electron microscope (TEM) with an operating voltage of 120 kV or a Philips 505 scanning electron microscope (SEM).

4. Experimental results

4.1. Creep behavior in the unreinforced and the reinforced materials

Representative creep data are shown in Figs 3 and 4 for the unreinforced AZ91 alloy and the AZ91 composite, respectively: all of these plots were obtained at an absolute temperature, T, of 473 K over a range of values of the applied stress, σ, and they show (a) the variation of the strain, ε, with the time, t, (b) the variation of the instantaneous strain rate, $\dot{\varepsilon}$, with the time and (c) the variation of the instantaneous strain rate with the strain.

Several important conclusions may be reached from inspection of these data. First, it is important to note there is an order of magnitude difference in the strain levels for Figs 3a and 4a so that the total strains achieved in the composite are very small by comparison with the strains achieved in the unreinforced matrix alloy. Thus, the specimens of the unreinforced AZ91 alloy recorded in Fig. 3a pull out to failure at strains of $\geq$0.10 whereas the composite specimens fail at strains of the

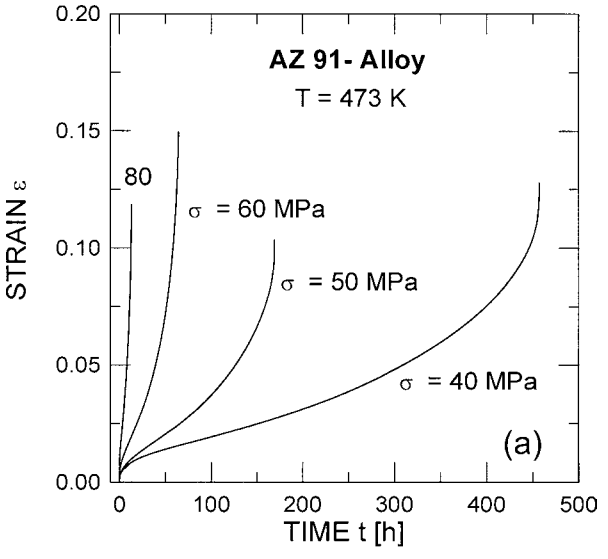

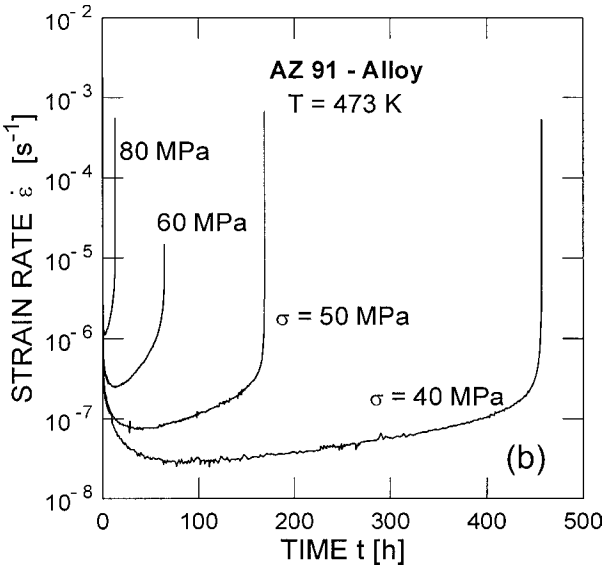

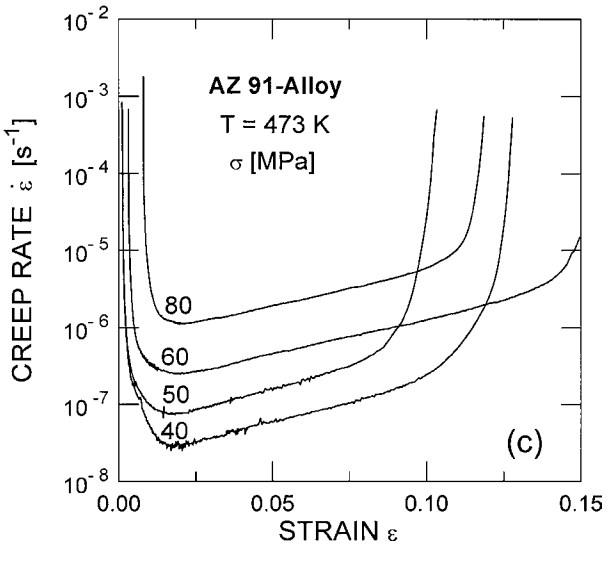

Figure 3 Creep results for the unreinforced AZ91 alloy showing: (a) creep curves of strain versus time, (b) the variation of strain rate with time and (c) the variation of strain rate with strain.

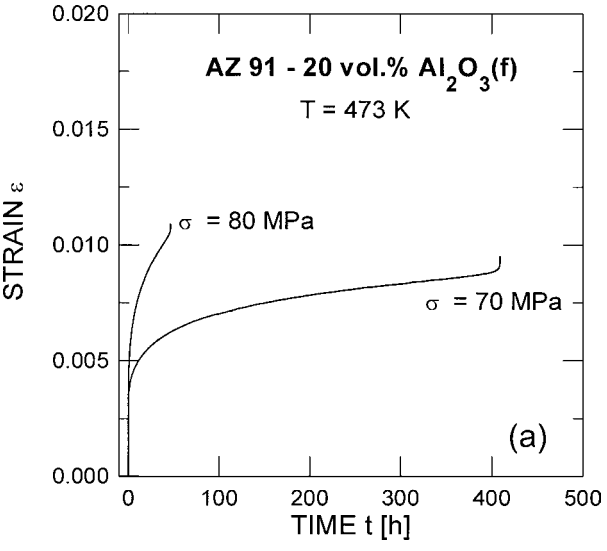

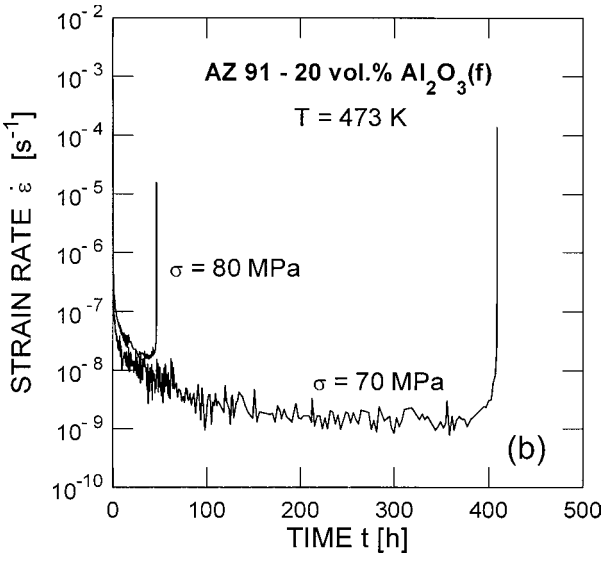

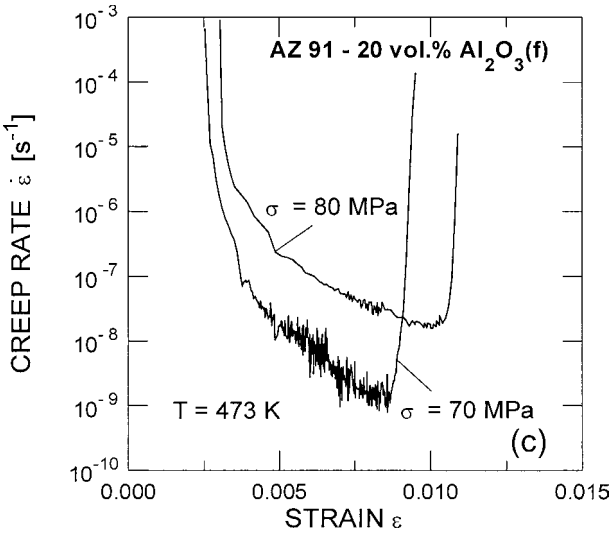

Figure 4 Creep results for the reinforced AZ91 composite showing: (a) creep curves of strain versus time, (b) the variation of strain rate with time and (c) the variation of strain rate with strain.

order of ∼0.01. Second, for constant values of the applied stress, it is apparent from Figs 3b and 4b that the composite exhibits markedly longer times to failure and, since the strain rate axes are different, the strain rates in the composite are thus markedly slower. Third, the fundamental creep curves are different in appearance between the unreinforced alloy and the composite, as illustrated in Fig. 3b and c and Fig. 4b and c where it is apparent there is only a quasi-secondary stage in the unreinforced alloy and in the composite there is little more than an abrupt minimum in the curves of

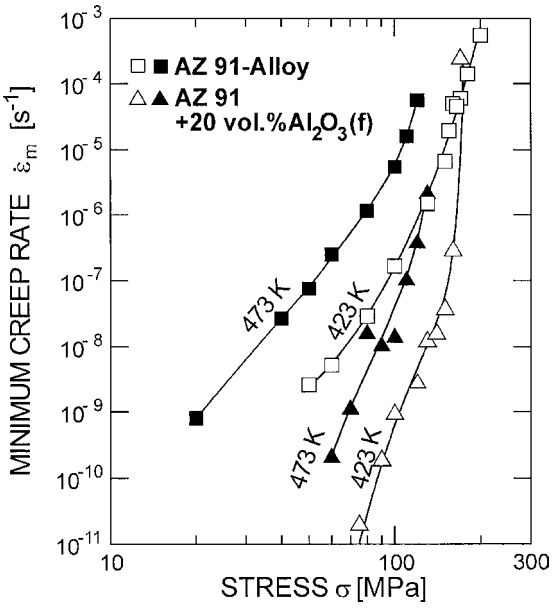

Figure 5 Minimum creep rate versus stress for the AZ91 alloy and the composite.

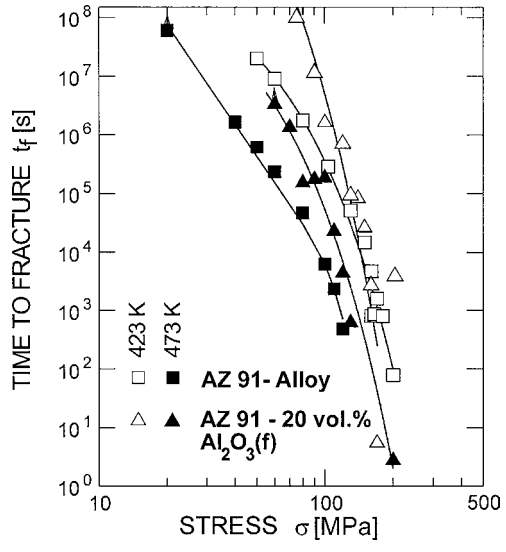

Figure 6 Time to fracture versus stress for the AZ91 alloy and the composite.

strain rate versus strain followed by a rapid acceleration to final failure. This difference is illustrated most readily in Figs 3c and 4c where it is apparent the creep behavior of the unreinforced alloy is dominated by a long and gradually accelerating tertiary stage whereas in the composite the creep behavior is dominated by a prolonged and extensive primary stage.

These differences are easily demonstrated by logarithmically plotting the minimum creep rate, $\dot{\varepsilon}_m$, against the stress as shown in Fig. 5 for tests conducted at the two temperatures of 423 and 473 K. Thus, the composite exhibits improved creep resistance, typically by >2 orders of magnitude, by comparison with the unreinforced alloy and, furthermore, the trend in these plots is different because the unreinforced alloy exhibits a decreasing value in the stress exponent, n, at the lower stresses whereas the composite exhibits a higher value of n with decreasing stress.

The increase in n at the lower stresses in the composite is a fundamental property of many metal matrix composites [17] and it is generally associated with the presence of a threshold stress marking a lower limiting stress below which no measurable strain rate can be achieved [18]. The data for the unreinforced alloy suggest a transition to a value of n close to ∼3 at the lower stress levels and this is consistent with earlier analyses of creep data for a composite with an AZ91 matrix [8] and data for an unreinforced AZ91 alloy [19]. It is consistent also with results obtained recently on the unreinforced AZ91 alloy using acoustic emission [20]. A value of $n = 3$ suggests that viscous glide is the rate-controlling mechanism in the matrix alloy and the increase in n at the higher stresses is then due to the breakaway of the dislocations from their solute atmospheres [15].

Fig. 6 shows the variation of the time to fracture, t_f, with the applied stress for the specimens tested at 423 and 473 K. These results demonstrate the creep lifetimes of the composite may be up to one order of magnitude longer than for the unreinforced alloy although this difference decreases with increasing applied stress so that, ultimately, there is very little difference at stresses greater than ∼150 MPa.

4.2. Microstructural characteristics after creep

It is possible to obtain some information on the mechanisms associated with creep and fracture by inspection of the micrographs shown in Figs 7 and 8 for

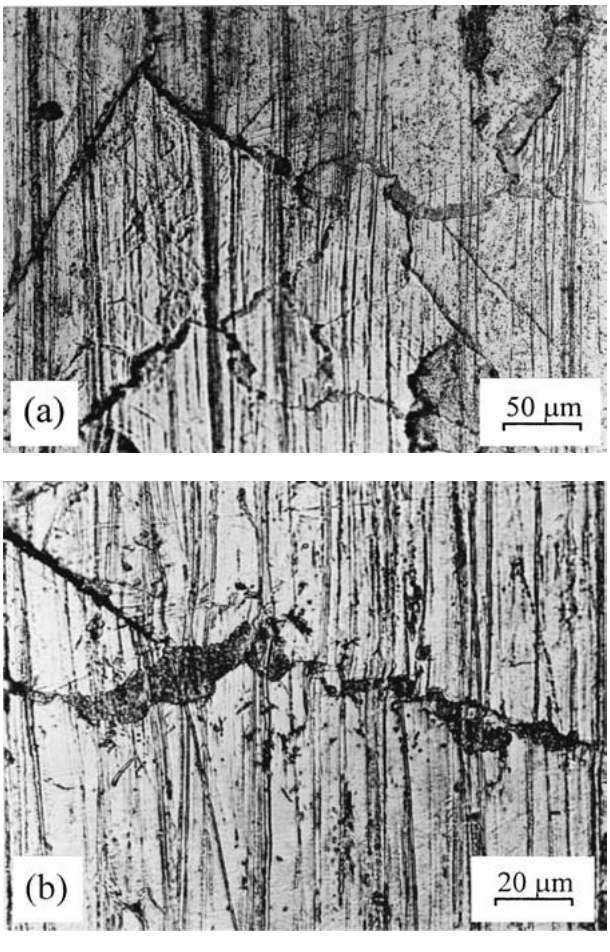

Figure 7 (a) and (b) Examples of grain boundary sliding in the AZ91 alloy after testing at 473 K and 40 MPa.

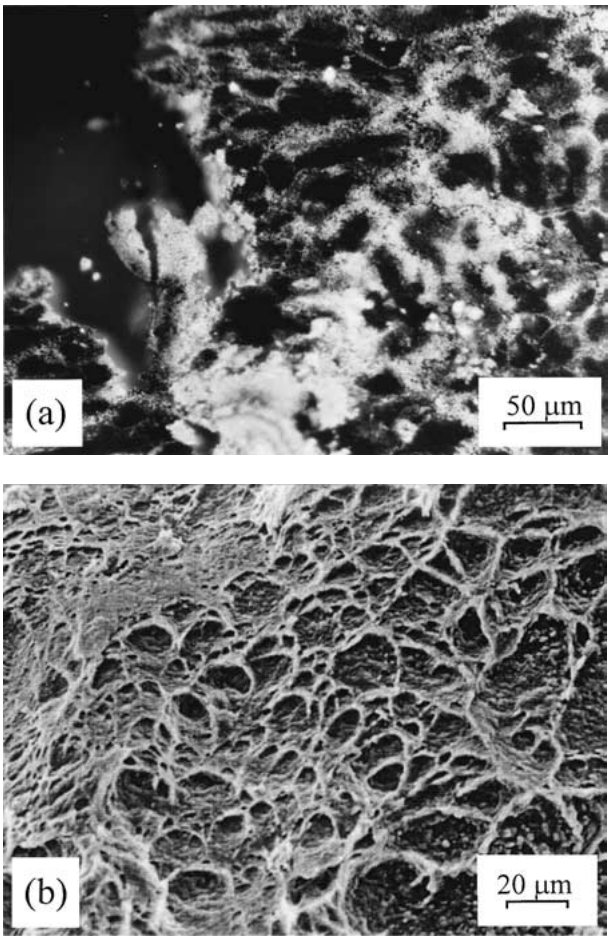

Figure 8 Intergranular creep fracture in the unreinforced AZ91 alloy: (a) optical micrograph of the fracture surface and (b) the creep fracture surface (SEM) after testing at 473 K and 50 MPa.

the unreinforced alloy and Fig. 9 for the composite, respectively. Fig. 7a and b show two clear examples of the occurrence of grain boundary sliding in the unreinforced alloy, where these two samples were tested at a temperature of 473 K under an applied stress of 40 MPa: in both examples, the tensile axes are horizontal and the transverse marker lines are clearly displaced at the grain boundaries. In practice, however, detailed measurements showed the overall contribution of sliding to the overall strain was very small, typically $<3\%$, primarily because the fraction of boundaries revealing measurable offsets was $<10\%$ and there was a large grain size in the unreinforced alloy ($\sim 200\ \mu$m). These measurements therefore support the well-established trend that high sliding contributions require fairly small grain sizes [21]. Fig. 8a and b show a typical fracture path and an intergranular creep fracture surface in the unreinforced alloy for a sample tested at 473 K under a stress of 50 MPa.

Representative micrographs for the composite are shown in Fig. 9 using light microscopy, TEM and SEM. In Fig. 9a for a sample tested at 473 K and 70 MPa, it is apparent there is an absence of any significant cracking of the fibers during creep testing. This is consistent with a similar report in an earlier study [22]. In addition, it appears for the same specimen in Fig. 9b that there is also no debonding between the fibers and

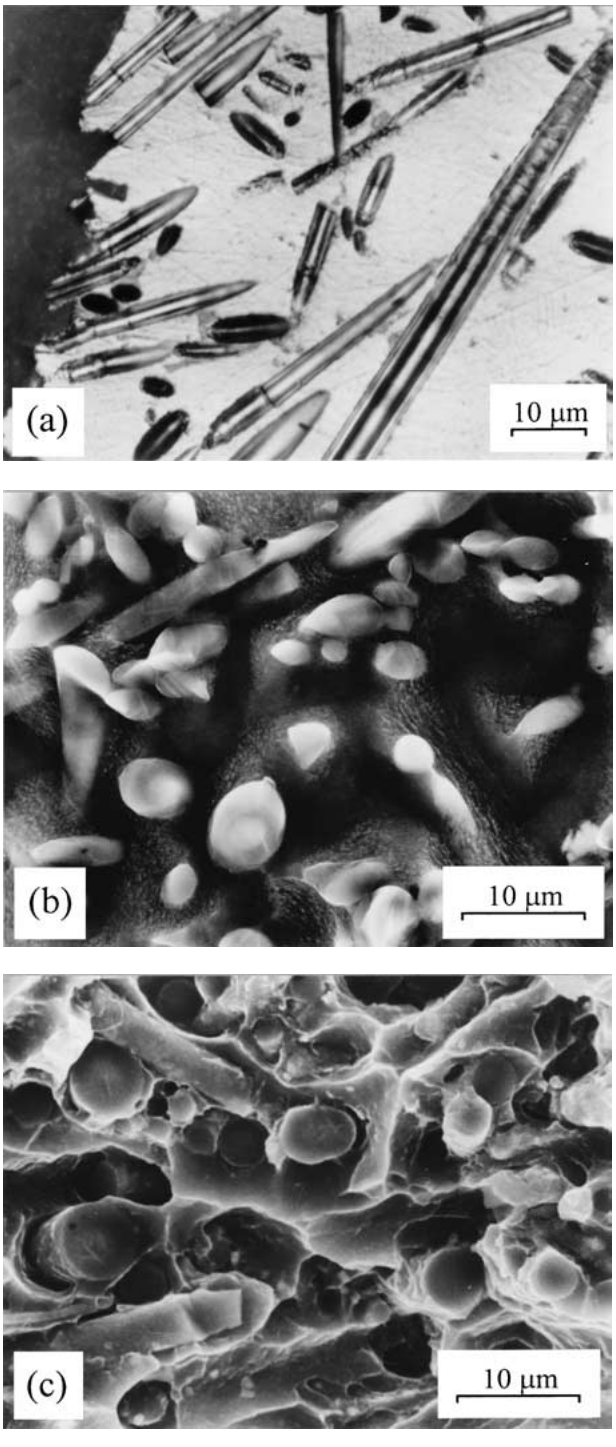

Figure 9 Evidence for an absence of: (a) cracking, (b) debonding in the AZ91 composite and (c) the creep fracture surface after testing at 473 K and 70 MPa.

the matrix alloy. Fig. 9c shows the fracture surface of this specimen and it appears that fiber breakage occurs as a consequence of the propagation of the main fracture crack through the material immediately prior to failure.

5. Discussion

The creep data in Fig. 5 suggest the presence of a threshold stress in the composite material. It is therefore appropriate to extend the analysis by determining the magnitudes of the threshold stresses at 423 and 473 K. It has been shown that threshold stresses may be estimated by

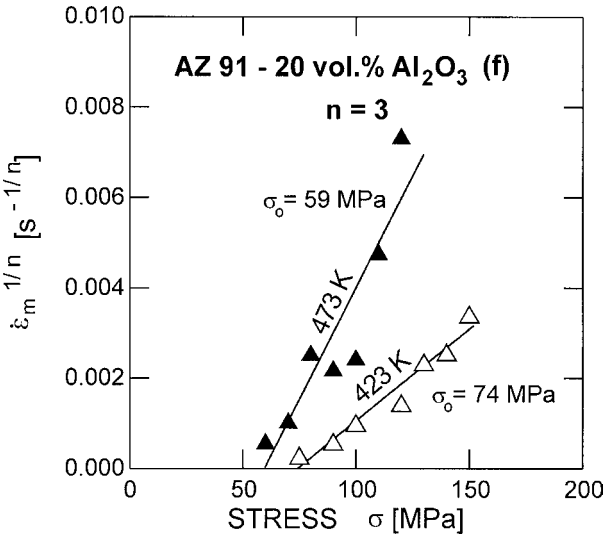

Figure 10 Procedure for determining the threshold stresses in the composite at 423 and 473 K using a stress exponent of $n = 3$.

extrapolating extensive sets of creep data to strain rates where the plots lie vertical [23] but in practice the data for the composite in Fig. 5 are insufficient to make use of this procedure since there are only a small number of experimental points delineating the occurrence of an increase in n at the very lowest stresses. Accordingly, it is necessary to use an alternative procedure in which the datum points are plotted, on linear axes, in the form of the strain rate raised to a power of $1/n$ against the values of the applied stress and then the results are linearly extrapolated to give the threshold stresses at a zero strain rate [24]. Thus, taking a value of $n = 3$ for control by a viscous glide process, Fig. 10 shows plots for the composite for the two different testing temperatures. Extrapolating these lines to zero strain rate, the two threshold stresses are estimated as $\sim$74 and $\sim$59 MPa for testing temperatures of 423 and 473 K, respectively.

Finally, it is necessary to consider the origin of the significantly greater creep resistance exhibited by the composite. This creep resistance may arise in two separate ways [25, 26]. First, because of a load transfer effect in which part of the external load is carried by the reinforcement. Second, by a substructural strengthening effect due to features such as the increased dislocation density which is present in the composite because of the thermal mismatch between the matrix and the reinforcement. Both of these processes probably make a contribution to the increase in strength but in practice it is difficult to estimate the separate contributions from these two factors.

Acknowledgements

This work was supported by the Academy of Sciences of the Czech Republic under Project K 1010104. The authors acknowledge Drs. M. Pahutová, K. Kuchařová and M. Svoboda, Institute of Physics of Materials ASCR, for their technical assistance.

References

1. G. F. WEISMANN and W. BABINGTON, *Proc. ASTM* **58** (1958) 869.
2. F. H. FROES, D. ELIEZER and E. AGHION, *JOM* **50**(9) (1998) 30.
3. K. JOHNSON, *Adv. Mater. Proc.* **160**(6) (2002) 62.
4. A. A. LUO, *Mater. Sci. Forum* **419–422** (2003) 57.
5. H. FRIEDRICH and S. J. SCHUMANN, *Mater. Proc. Tech.* **117** (2001) 276.
6. B. L. MORDIKE, *Mater. Sci. Eng.* A **324** (2002) 103.
7. B. L. MORDIKE and P. LUKÁČ, *Surf. Interf. Anal.* **31** (2001) 682.
8. Y. LI and T. G. LANGDON, *Metall. Mater. Trans.* A **30A** (1999) 2059.
9. V. SKLENIČKA, M. SVOBODA, M. PAHUTOVÁ, K. KUCHAŘOVÁ and T. G. LANGDON, *Mater. Sci. Eng.* A **319–321** (2001) 741.
10. M. SVOBODA, M. PAHUTOVÁ, K. KUCHAROVÁ, V. SKLENIČKA and T. G. LANGDON, *ibid.* A **324** (2002) 151.
11. V. SKLENIČKA, M. PAHUTOVÁ, K. KUCHAŘOVÁ, M. SVOBODA and T. G. LANGDON, *Metall. Mater. Trans.* A **33A** (2002) 883.
12. S. S. VAGARALI and T. G. LANGDON, *Acta Metall.* **29** (1981) 1969.
13. T. G. LANGDON, *Metall. Mater. Trans.* A **33A** (2002) 249.
14. F. A. MOHAMED and T. G. LANGDON, *Acta Metall.* **22** (1974) 779.
15. P. YAVARI and T. G. LANGDON, *ibid.* **30** (1982) 2181.
16. S. S. VAGARALI and T. G. LANGDON, *ibid.* **30** (1982) 1157.
17. Y. LI and T. G. LANGDON, *Metall. Mater. Trans.* A **30A** (1999) 315.
18. J. C. GIBELING and W. D. NIX, *Mater. Sci. Eng.* **45** (1980) 123.
19. W. BLUM, P. WEIDINGER, B. WATZINGER, R. SEDLAČEK, R. RÖSCH and H.-G. HALDENWANGER, *Z. Metallkd.* **88** (1997) 636.
20. F. CHMELIK, P. LUKÁČ, M. JANEČEK, F. MOLL, B. L. MORDIKE, K.-U. KAINER and T. G. LANGDON, *Mater. Sci. Eng.* A **338** (2002) 1.
21. R. L. BELL and T. G. LANGDON, *J. Mater. Sci.* **2** (1967) 313.
22. M. PAHUTOVÁ, J. BŘEZINA, K. KUCHAŘOVÁ, V. SKLENIČKA and T. G. LANGDON, *Mater. Lett.* **39** (1999) 179.
23. Y. LI and T. G. LANGDON, *Scripta Mater.* **36** (1997) 1457.
24. R. LAGNEBORG and B. BERGMAN, *Metal Sci.* **10** (1976) 20.
25. Y. LI and T. G. LANGDON, *Acta Mater.* **47** (1999) 3395.
26. B. Q. HAN and T. G. LANGDON, *Mater. Sci. Eng.* A **322** (2002) 73.

Received 15 April
and accepted 13 November 2003